DOI: 10.1002/chem.200901753

Ambident PCN Heterocycles: N- and P-Phosphanylation of Lithium 1,3-Benzazaphospholides

Bhaskar R. Aluri,[a] Sebastian Burck,[b] Dietrich Gudat,*[b] Mark Niemeyer,[c] Oldamur Holloczki,[d] Laszlo Nyulaszi,*[d] Peter G. Jones,[e] and Joachim Heinicke*[a]

Dedicated to Professor Reinhard Schmutzler on the occasion of his 75th birthday

Abstract: Synthetic and structural aspects of the phosphanylation of 1,3-benzazaphospholides $\mathbf{1_{Li}}$, ambident benzofused azaphosphacyclopentadienides, are presented. The unusual properties of phospholyl-1,3,2-diazaphospholes inspired us to study the coupling of $\mathbf{1_{Li}}$ with chlorodiazaphospholene **2**, which led to the N-substituted product **3**. Reaction of $\mathbf{1_{Li}}$ with chlorodiphenyl- and chlorodicyclohexylphosphane likewise gave *N*-phosphanylbenzazaphospholes **4** and **5**, whereas with the more bulky di-*tert*-butyl- and di-1-adamantylchlorophosphanes, the diphosphanes **6** and **7** are obtained; in the case of **7** they are isolated as a dimeric LiCl(THF) adduct. Structural information was provided by single-crystal X-ray diffraction and solution NMR spectroscopy experiments. 2D exchange spectroscopy confirmed the existence of two rotamers of the aminophosphane **5** at room temperature; variable-temperature NMR spectroscopy studies of **6** revealed two dynamic processes, low-temperature inversion at ring phosphorus ($\Delta H^{\neq} = 22\ \mathrm{kJ\,mol^{-1}}$, $\Delta S^{\neq} = 2\ \mathrm{J\,K^{-1}\,mol^{-1}}$) and very low-temperature rotation of the $t\mathrm{Bu_2P}$ group. Quantum chemical studies give evidence that 2-unsubstituted benzazaphospholides prefer N-phosphanylation, even with bulky chlorophosphanes, and that substituents at the 2-position of the heterocycle are crucial for the occurrence of P–N rotamers and for switching to alternative P-substitution, beyond a threshold steric bulk, by both P- and 2-position substituents.

Keywords: ambident reactivity · dynamic processes · heterocycles · phosphanes · quantum chemistry

Introduction

Azaphospholides with one[1] or more nitrogen atoms[2,3] in the ring are structurally related to the cyclopentadienide anions.[4] Their reactivity, however, is controlled by the heteroatoms. Computations on gas-phase structures show that lithium 1,3-azaphospholide is η^5-coordinated.[5] In the presence of donor solvents—for example, THF—lithium coordi-

[a] Dr. B. R. Aluri, Prof. Dr. J. Heinicke
Institut für Biochemie—Anorganische Chemie
Ernst-Moritz-Arndt-Universität Greifswald
Felix-Hausdorff-Strasse 4, 17487 Greifswald (Germany)
Fax: (+49) 3834-864377
E-mail: heinicke@uni-greifswald.de

[b] Dr. S. Burck, Prof. Dr. D. Gudat
Institut für Anorganische Chemie
Universität Stuttgart
Pfaffenwaldring 55, 70550 Stuttgart (Germany)
E-mail: gudat@iac.uni-stuttgart.de

[c] Dr. M. Niemeyer
Institut für Anorganische und Analytische Chemie
Johannes Gutenberg-Universität Mainz
Duesbergweg 10–14, 55128 Mainz (Germany)

[d] O. Holloczki, Prof. Dr. L. Nyulaszi
Department of Inorganic Chemistry
Technical University of Budapest, 1521 Budapest (Hungary)
E-mail: Nyulaszi@mail.bme.hu

[e] Prof. Dr. P. G. Jones
Institut für Anorganische und Analytische Chemie
Technische Universität Braunschweig
Hagenring 30, 38106 Braunschweig (Germany)

Supporting information for this article is available on the WWW under http://dx.doi.org/10.1002/chem.200901753. It includes ^{31}P and ^{13}C NMR spectroscopic data, determination of activation enthalpy and entropy for the inversion at the ring phosphorus atom in **6**, details on quantum chemical calculations, and detailed X-ray structural data of **1**, **3**, **5**, and **7**.

nates preferably at nitrogen, as shown by crystal-structure analysis of a more easily accessible lithium 1,3-benzazaphospholide THF trisolvate, that exhibits only a marginal upfield phosphorus resonance ($\Delta\delta < 10$ ppm) with respect to the uncomplexed system. Zero-valent Group 6 metal carbonyls bind at phosphorus.[6] The reactivity towards non-zero-valent metal and other electrophilic compounds is different for mono- and di- or triazaphospholides. Whereas the latter prefer reaction at a basic dicoordinate nitrogen atom,[2,3] the 1,3-azaphospholides[1] and benzazaphospholides[6,7] display ambident reactivity that was interpreted by simple hard and soft acid and base (HSAB) considerations. The real behavior is, however, more subtle and depends also on steric factors, as seen by the different sites of trimethylsilylation in various 2-substituted 1,3-benzazaphospholides[6a] and in analogous arsenic heterocycles.[8] Reactions of such anions with chlorophosphanes are not yet known. Only the sparingly characterized *N*-dichlorophosphanylbenzazaphosphole, formed by prolonged reflux of neat 1*H*-1,3-benzazaphosphole in excess PCl_3, was reported. Attempts at coupling with R_2PCl failed,[7] whereas di- and triazaphospholes undergo clean N-substitution without metalation.[9] To shed more light on the behavior of the P,N-heterocyclic anions and the nature of phosphanylation products, the reactivity of an easily accessible lithium benzazaphospholide $\mathbf{1_{Li}}$ towards selected chlorophosphanes was studied.

Apart from the regioselectivity problem, *N*- and *P*-phosphanyl-1,3-benzazaphospholes are of interest because of the different electronic structure and properties of the 1*H*- and 3*H*-1,3-benzazaphosphole systems.[10] In 1-phosphanyl-1,3-benzazaphospholes, the nitrogen lone pair is still part of the delocalized π system, which is expected to cause weakening of the P–N bond compared with ordinary aminophosphanes. In contrast, 3-phosphanyl-1,3-benzazaphospholes featuring a pyramidal phosphorus atom should be destabilized by a loss of aromaticity. Furthermore, the P–P bond strength differs from that of the P–N bond, and also the P=C and N=C double-bond energies are different. P–P bond polarization, however, with concomitant buildup of negative partial charge at the ring phosphorus atom, might allow for some residual stabilization by weak π interactions. An effect of this type has been observed for 2-phospholyl-1,3,2-diazaphospholenes, which display perceptible lengthening of the P–P bond in connection with an increased bond ionicity[11] and are consequently highly reactive in insertion reactions into polar single[12] and multiple bonds.[13] To find out if the corresponding benzazaphospholyldiazaphospholenes prefer N–P- or P–P-bonded structures, we have extended our study to include coupling of $\mathbf{1_{Li}}$ with 2-chloro-1,3-dimesityl-4,5-dimethyl-1,3,2-diazaphospholene (**2**)[14] and present the spectroscopic and structural characterization of the product, together with a computational study of structural aspects and relative stabilities of *N*- or *P*-phosphanyl-substituted 1,3-benzazaphospholes.

Results and Discussion

2,5-Dimethyl-1*H*-1,3-benzazaphosphole (**1**) was synthesized by nickel-catalyzed phosphonylation of commercially available 2-bromo-4-methylacetanilide and subsequent reductive cyclization with excess $LiAlH_4$, the shortest route to these 1*H*-1,3-benzazaphospholes.[15] Lithiation was performed by using *tert*-butyllithium at low temperature in THF. Under these conditions the bulky lithium reagent prefers NH metalation to addition at the P=C bond. Lithiation by $LiNEt_2$[7] or lithium diisopropylamide (LDA)[8] is less suitable, as it requires complete removal of Et_2NH or iPr_2NH to avoid competing reactions with chlorophosphanes. The conversion of **1** with the chloro-1,3,2-diazaphospholene **2** took place with high selectivity at nitrogen and furnished crystalline benzazaphosphol-1-yl-diazaphospholene **3** in good yield (Scheme 1). The increased polarity and reactivity of the Cl–P bond of **2**[14] may have contributed to the clean course of the reaction.

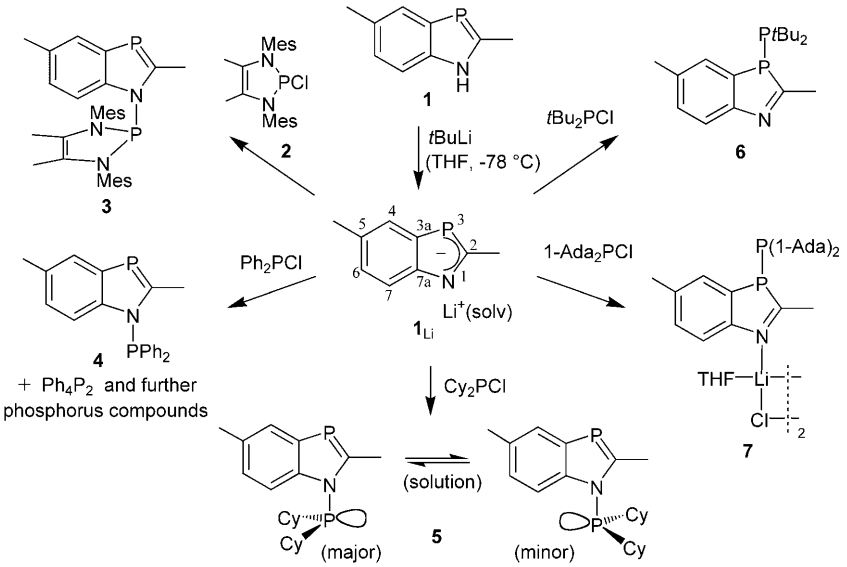

Scheme 1. Lithiation of **1** and coupling of $\mathbf{1_{Li}}$ with chlorophosphanes.

To find out whether chlorophosphanes generally prefer substitution of $\mathbf{1_{Li}}$ at nitrogen, or if this is governed by electronic and/or steric effects, the investigation was extended to coupling of $\mathbf{1_{Li}}$ with Ph_2PCl, Cy_2PCl, tBu_2PCl, and 1-Ada_2PCl (Cy = cyclohexyl; Ada = adamantyl) as representa-

tives of diaryl- and dialkylchlorophosphanes with varying steric bulk. The reaction of $\mathbf{1_{Li}}$ and chlorodiphenylphosphane did not proceed in a well-defined way (at −78 °C) and provided a mixture of products. NMR spectroscopic analysis of the crude material, obtained by removal of the solvent and extracting the residue with diethyl ether, revealed roughly 40 mol % of **4** (by integration of Me proton signals), accompanied by about the same amount of recovered **1**. Smaller ^{31}P signals indicated tetraphenyldiphosphane and two unknowns each with 50 % of the intensity of the former and phosphorus resonances in the (3*R*)-benzazaphosphole range ($\delta(^{31}P) = -5.55, -5.74$ ppm).

Chlorodicyclohexylphosphane reacted, like **2**, in an unambiguous way. The yield of the product was somewhat lower, and in the NMR spectra two sets of signals were observed, but both belong to the N-substitution product **5** and form two stable rotamers (see below). Thus, the selectivity was preserved. However, increase of the steric bulk changes this preference. Chloro-di-*tert*-butylphosphane and $\mathbf{1_{Li}}$ react under the same conditions as used in the aforementioned couplings and with similar yield, but with attack at phosphorus and formation of **6**. The further increased steric congestion in chlorobis(1-adamantyl)phosphane leads to the same preference for reaction at phosphorus but very slow conversion. Reaction monitoring by ^{31}P NMR spectroscopy revealed that the major part of the starting materials was converted only after three weeks at room temperature. Whereas **6** was isolated as a colorless oil by high vacuum distillation (after extraction with hexane from the crude mixture), analogous workup of the 3-diadamantylphosphanylbenzazaphosphole **7** failed and furnished only decomposition products. However, layering of the concentrated solution of the crude product in THF with hexane led to isolation of a N-coordinated LiCl(THF) adduct, the crystalline chloro-bridged dimer $[\mathbf{7}\cdot\mathrm{LiCl(thf)}]_2$.

Both *N*- and *P*-phosphanyl-1,3-benzazaphospholes are highly sensitive to moisture and are attacked by any trace of water with formation of **1** and R_2PHO, easily detectable by ^{31}P NMR spectroscopy. Thus, **6** is cleaved to give **1** and $t\mathrm{Bu_2PHO}$ ($\delta(^{31}P) = 73.5$ and 61.9 ppm). The strongly increased reactivity of the P–N bond relative to common aminophosphanes and the easy hydrolysis of the normally nonpolar P–P bond suggests weakened and/or strongly polarized or polarizable P–N and P–P bonds.

Table 1. Selected bond lengths [Å] and angles [°] of the benzazaphosphole ring in **1**, **3**, **5**, and **7**.

Compound	**1**	**3**	**5**	$[\mathbf{7}\cdot\mathrm{LiCl(thf)}]_2$[a]
P–C2	1.7284(13)	1.719(3)	1.714(2)	1.8190(16)
P–C3A	1.7934(12)	1.783(3)	1.789(2)	1.8041(16)
N–C2	1.3694(16)	1.394(4)	1.386(2)	1.305(2)
N–C7A	1.3799(15)	1.415(3)	1.410(2)	1.418(2)
N–P_{subN}	–	1.812(2)	1.7622(15)	–
N–Li	–	–	–	2.135(3)
C3A–C7A	1.4128(15)	1.404(4)	1.406(3)	1.404(2)
N-C2-P	113.20(9)	115.5(2)	115.30(14)	114.58(12)
N-C7A-C3A	112.01(11)	112.7(2)	112.44(16)	116.89(14)
P-C3A-C7A	110.67(9)	111.8(2)	111.45(14)	107.97(12)
C2-N-C7A	114.60(10)	110.9(2)	111.66(15)	111.29(13)
C2-P-C3A	89.52(6)	89.03(14)	89.09(9)	88.45(7)
N-C2-C_{Me}	118.50(11)	121.8(2)	120.99(17)	121.85(14)
P-C2-C_{Me}	128.30(10)	122.7(2)	123.70(15)	123.19(11)
P_{subN}-N-C2 or Li-N-C2	–	118.05(18)	119.94(13)	124.65(14)
P_{subN}-N-C7A or Li-N-C7A	–	130.68(19)	127.51(13)	–
	–	–	–	123.88(13)
P_{subP}-P-C2	–	–	–	104.97(5)
P_{subP}-P-C3A	–	–	–	117.97(5)
P–N or P–C (substituent)	–	1.706(2), 1.707(2)	1.8549(19), 1.8563(19)	1.8896(16), 1.8934(16)
N-P-N or C-P-C (substituent)	–	89.99(11)	106.27(8)	112.09(7)
N_{BAP}-P-N{or C} [P_{BAP}-P-C]	–	104.62(11), 105.54(11)	{100.92(8), 103.48(8)}	[98.15(5), 109.52(5)]

[a] P3–P1 2.2025(6) Å.

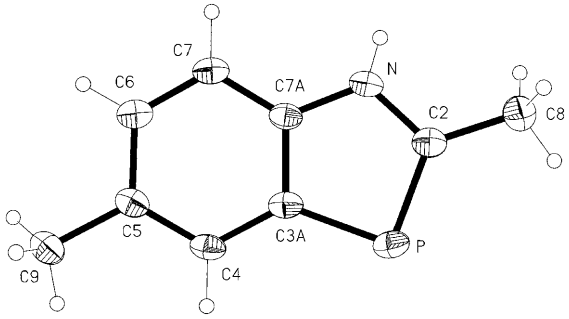

Figure 1. Crystal structure of **1**. Ellipsoids represent 50 % probability levels. Selected bond lengths [Å] and angles [°]: P–C2 1.7284(13), P–C3A 1.7934(12), C2–N 1.3694(16), N–C7A 1.3799(15), C3A–C7A 1.4128(15); N-C(2)-P 113.20(9), C(2)-P-C(3A) 89.52(6).

Structural aspects: The molecular structures of **3**–**7** were confirmed unambiguously by characteristic or full sets of solution NMR spectroscopic data. For more detailed information, the crystal structures of **1**, **3**, **5**, and **7** have been determined. Compound **1** was included to visualize the changes in bond lengths and angles (Table 1) caused by the N- or P-substituents. Finally, NMR spectroscopic studies of **5** and **6** addressing the occurrence of rotamers and dynamic behavior in solution were performed.

Crystal structures: The molecular structure of compound **1** (Figure 1) shows the expected planar benzazaphosphole ring system (mean deviation 0.03 Å). Bond lengths and angles are comparable to those in other 1*H*-1,3-benzazaphospholes.[15a,16] The 2-methyl group is slightly bent towards the N atom (N-C2-C8 118.50(11)° versus P-C2-C8 128.30(10)°), but does not severely hinder access to the nitrogen atom in the metalation and substitution reactions, except by very bulky electrophiles.

The benzazaphospholyldiazaphospholene **3** cocrystallizes with one molecule of deuterobenzene. The molecular structure (Figure 2) confirms bonding of the diazaphospholene unit to the nitrogen atom of the azaphosphole ring and shows that the planarity of the benzazaphosphole is con-

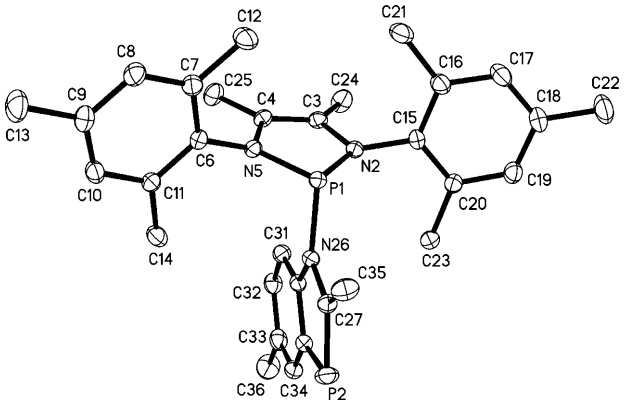

Figure 2. Molecular structure of $\mathbf{3}\cdot C_6D_6$ in the crystal. Ellipsoids represent 30% probability levels. Hydrogen atoms and the cocrystallized deuterobenzene molecule have been omitted for clarity.

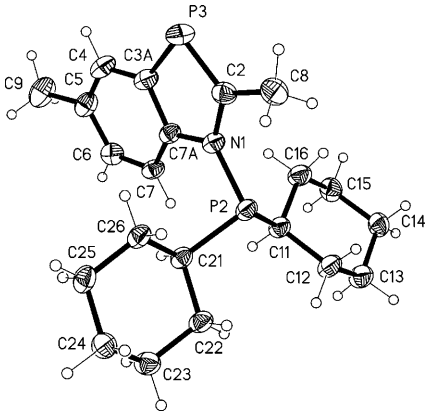

Figure 3. Molecular structure of **5** in the crystal. Ellipsoids represent 50% probability levels.

served (average deviation 0.03 Å). The shape of the diazaphospholene ring resembles that in other amino-substituted diazaphospholenes[17] and is not strictly planar in contrast to genuine diazaphospholenium cations.[14] The phosphorus atom lies 0.055 Å above the N5-C4-C3-N2 plane towards the benzazaphosphole group, and the exocyclic P–N bond, which forms an angle of 71° to the N5-C4-C3-N2 plane, fixes the diazaphospholene ring like a bisecting roof (N2-P1-N26-C27 130.5(2)° versus N5-P1-N26-C27 −135.5(2)°) over the benzazaphosphole ring. The planar mesityl groups are arranged with dihedral angles of −77.1(3) and 65.3(4)° for C4-N5-C6-C7 and C3-N2-C15-C16, respectively. The exocyclic P–N bond (1.812(2) Å) is considerably longer than the P–N bonds within the ring (Table 1) and also slightly longer than the comparable exocyclic P–N bond of a pyrazolyldiazaphospholene (1.798(2) Å).[17] The lengthening relative to the exocyclic P–N bond in **5** reflects a local bond weakening in favor of electronic stabilization within the diazaphospholene ring. Geometry and bond lability resemble those of adducts of neutral N-heterocyclic carbenes (Lewis base) at N-heterocyclic silylenes, germylenes, or stannylenes (here acting as Lewis acids).[18] Compound **5**, depicted in Figure 3, also displays an essentially planar heterocyclic system (mean deviation 0.03 Å); it bears an electronically indifferent PCy_2 group at nitrogen, arranged in a similar bisecting conformation (C11-P2-N3-C2 −126.45(15)° versus C21-P2-N3-C2 123.70(14)°) with the P2–C11 and P2–C21 bonds on different sides of the benzazaphosphole plane and directed towards the benzo-end of the bicyclic ring system. Compared with **1** the C–N bonds of the azaphosphole ring are similarly elongated in **3** and **5**, and the P–C and C–C bonds are slightly shortened. In the anionic $\mathbf{1}_{Li}$,[6a] however, the changes with respect to **1** are different. Finally it should be mentioned that introduction of N-substituents causes slight elongation of the P-C-N and N-C-C(Me) angles and reduction of the C-N-C angles (Table 1).

The P-substituted benzazaphoshole **7** crystallized coordinated to LiCl(THF). The molecule (Figure 4) forms an inversion-symmetric dimer with an Li_2Cl_2 rhombus. The deviations from planarity within the benzazaphosphole ring are again small (mean deviation 0.03 Å); the configuration at P3 is distorted pyramidal (angle sum 311.4°). The dihedral angles N1-C2-P3-P1 127.45(11)° and P1-P3-C3A-C7A −113.12(10)° correspond to the direction of the P3–P1 bond out of the azaphosphole plane, whereas the dihedral angles around the P–P axis show that one adamantyl group is arranged nearly eclipsed to C3A (C3A-P3-P1-C11 17.10(8)°) and the other nearly *anti* to C2 (C2-P3-P1-C21 163.78(7)°).

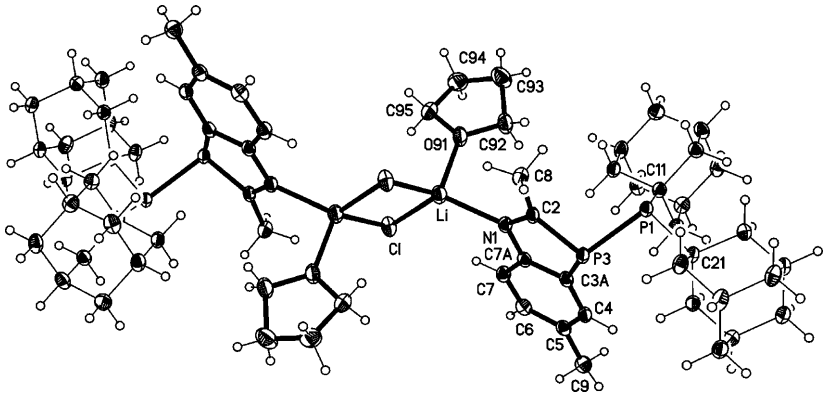

Figure 4. Molecular structure of $[\mathbf{7}\cdot LiCl(thf)]_2$ in the crystal. Ellipsoids represent 50% probability levels. Selected bond lengths [Å] and angles [°]: O(91)-Li-N(1) 98.01(13), O(91)-Li-Cl 107.76(13), O(91)-Li-Cl#1 109.92(14), N(1)-Li-Cl 122.22(14), N(1)-Li-Cl#1 120.17(13), Cl#1-Li-Cl 98.36(11), Li#1-Cl-Li 81.64(11); further data in Table 1.

The P3–P1 bond length (2.2025(6) Å) lies in the normal range for diphosphanes ((2.217 ± 0.08) Å[11]), with the P3–C3A bond slightly lengthened and the P3–C2 bond appreciably lengthened relative to that in **1**, whereas the N1–C2 bond is markedly shortened. These bond lengths correspond to the usual (3*R*)-benzazaphosphole structure. This, together with the thermal stability of **6**, suggests that the sensitivity of **6** and **7** towards moisture may be caused by an easier polarizability compared to normal diphosphanes.

Solution structures: The most characteristic data for establishing *N*- or *P*-phosphanylation by solution spectra of **3–7** are the phosphorus chemical shifts and P,P coupling constants. Compound **4** ($\delta = 92.9$ (P_{ring}), 40.5 ppm (PPh_2), $^3J = 7.0$ Hz), which could not be isolated in pure form, was unambiguously identified as a 1-diphenylphosphanylbenzazaphosphole by the small P,P coupling constant, which was definitely too small for a one-bond coupling, and the characteristic downfield shift of the ring-phosphorus resonance relative to **1** ($\Delta\delta = 21.1$ ppm), found also in **3** ($\Delta\delta = 18.7$ ppm), **5** (major rotamer $\Delta\delta = 13.4$ ppm, minor rotamer $\Delta\delta = 23.4$ ppm), and 1-trimethylsilylbenzazaphospholes.[6a] 3-Phosphanylated benzazaphospholes display upfield shifted doublets for the ring phosphorus nuclei and large one-bond P,P coupling constants (**6**: $\Delta\delta = -77.8$ ppm, $^1J_{P,P} = 425$ Hz; **7**: $\Delta\delta = -84.1$ ppm, $^1J_{P,P} = 418$ Hz). The observation of substantial line broadening for both doublets in the room temperature spectra of **6** and **7** was interpreted as a result of dynamic exchange broadening, which in the case of **6** was confirmed by a variable temperature (VT) NMR spectroscopic study (see below). The magnitude of the P,P coupling constants in **6** and **7** comes close to the value of $^1J_{P,P}$ in $t\mathrm{Bu_2P}$–$\mathrm{P}t\mathrm{Bu_2}$ (−451 Hz[19]), which is presumably a consequence of both steric bulk (as evidenced by the large C-P-C bond angles of 112.1(1)° for [**7**·LiCl(thf)]$_2$) and a high degree of s character in the P–P bond.[20] Conclusive information on the constitution in solution is also provided by the characteristic ^{13}C resonances and *J*(P,C) coupling constants. Thus, N- and P-substituted benzazaphospholes are clearly distinguished by the chemical shifts of C3A, C7A, and C7. Compared with the 1*H*-1,3-benzazaphosphole **1**, the signal of C3A is upfield shifted in (3*R*)- ($\Delta\delta \approx -14$–15 ppm) and slightly downfield shifted ($\Delta\delta \approx 1$–2 ppm) in (1*R*)-benzazaphospholes, whereas C7A and C7 are less deshielded in (1*R*)- ($\Delta\delta \approx 3$–6, 4–10 ppm) than in (3*R*)-benzazaphospholes ($\Delta\delta \approx 12$, 16 ppm). The effect of phosphanylation at N or P on the chemical shift of C2 is similar, ($\Delta\delta = 10$–12 ppm), but the ^1J(P,C) coupling remains much larger for the P=C–NR than the RP–C=N heterocycles.

Solutions of **5** display two sets of phosphorus and carbon signals at room temperature, each with similar chemical shifts and, except for the occurrence of clearly different values for ^3J(P,C) of C7 and 2-CH_3, with similar coupling constants. The minor isomer is distinguished by the observation of a large splitting for the signal of C7 (^3J(P,C) = 33.3 Hz), whereas the signal of 2-CH_3 appears as a singlet; both findings hint at a close proximity between the lone pair and C7[21] and suggest that the exocyclic PCy_2 moiety adopts an orientation in which the phosphorus lone pair remains close to the plane of the benzazaphosphole ring and points towards C7, and thus away from the 2-CH_3 group (cf. Scheme 1; this lone-pair orientation may also be held responsible for the observation of an additional splitting for the signals of the adjacent carbon nuclei C7A and C6, usually doublets by coupling with P3, to triplets). In the major isomer, the signal of C7 appears as a singlet and the methyl carbon as a doublet of doublets because of large couplings to both phosphorus atoms ($^{2,3}J = 27.4$, 31.4 Hz), thereby indicating that the orientation of the PCy_2 lone pair is now reversed. Altogether, these assignments allow us to attribute the two observable sets of signals to two different rotamers for which the half-life time is sufficiently large to give rise to distinguishable sets of NMR spectroscopic signals at room temperature. This hypothesis is further substantiated by the appearance of cross peaks that connect the appropriate signals of both rotamers in a 2D-EXSY (EXchange SpectroscopY) spectrum (see the Supporting Information) and confirm that both species are in dynamic equilibrium at room temperature. The slow rate of interconversion suggests a rotational barrier of considerable height, and evaluation of relative populations (integration of methyl ^{1}H NMR spectroscopic signals indicated a molar ratio of approximately 9:1 at 296 K). This implies that the orientation of the phosphorus lone pair towards the 2-methyl group and of the cyclohexyl substituents towards the benzene ring represents the more stable rotamer. Interestingly, the same orientiation of the PCy_2 group is also present in crystalline **5** and, based on the evaluation of ^3J(P,C) coupling constants, in solutions of **3**.

Low-temperature NMR spectroscopic studies of compound **6**: The above-mentioned dynamic behavior of **6** was studied in more detail by means of VTNMR spectroscopy experiments. Upon lowering the temperature, the ^{31}P signals become at first broader, then again sharper, and below −50 °C they split into two sets of signals with relative intensities of approximately 10:1. The proton signal of the $t\mathrm{Bu_2P}$ group, at room temperature a broad doublet, broadened upon cooling and then decoalesced into two signals of equal intensity. Below −50 °C, all proton signals split further into two sets of signals with relative intensities of approximately 10:1. The observed temperature dependence of both ^{1}H and ^{31}P NMR spectra can be explained by the occurrence of two dynamic processes, 1) inversion at the ring phosphorus atom, thereby inducing coalescence of the ^{1}H NMR spectroscopic signals of the two diastereotopic *tert*-butyl groups above −50 °C, and 2) freezing the rotation around the P–P bond at low temperature, thereby leading to decoalescence of all ^{1}H and ^{31}P NMR spectroscopic signals into two sets of resonances with unequal intensities, which are attributable to two distinguishable rotamers. The P-inversion process can be visualized by the appearance of strong cross peaks, with intensities comparable to those of the diagonal peaks, in 2D-EXSY spectra recorded below the coalescence tempera-

ture (Figure 5); line-shape analysis of ^{1}H NMR spectra recorded between 223 and 303 K allowed the determination of the activation parameters for this process as $\Delta H^{\neq} =$ 22 kJ mol^{-1} and $\Delta S^{\neq} = 2$ J K^{-1} mol^{-1}. The dynamic exchange between the two distinguishable rotamers formed after the P–P bond rotation is frozen is likewise evident from the appearance of positive exchange peaks between the signals at $\delta = 2.88/2.72$ ppm in the 2D-EXSY spectrum (see Figure 5); determination of activation parameters from line-shape analysis was in this case prevented as the lack of sufficient data in the slow-exchange regime prevented the determination of reliable chemical shifts for the individual rotamers.

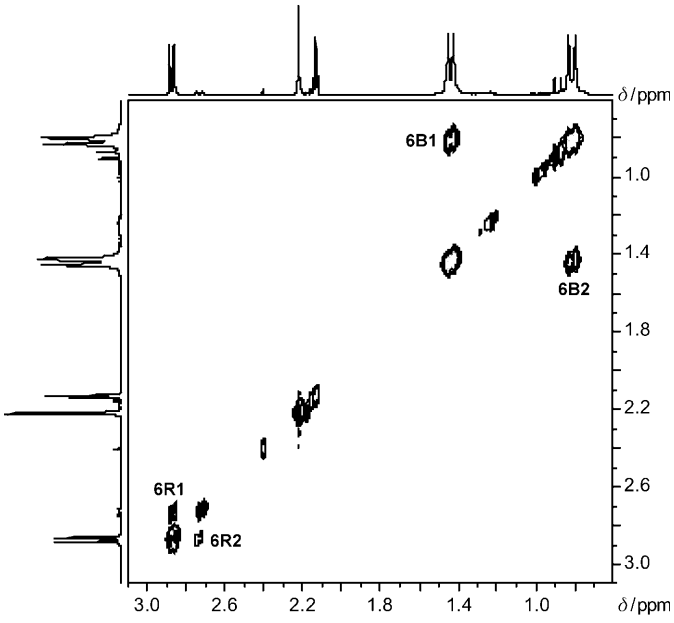

Figure 5. Expansion of a ^{1}H 2D-EXSY spectrum of **6** (213 K, mixing time 300 ms, only positive contour levels shown). Signals of P(tBu)$_2$ substituents are denoted as **6B1** and **6B2**, and 2-CH$_3$ resonances of the distinguishable rotamers as **6R1** and **6R2** (tBu signals of individual rotamers are not yet visible as the temperature is still above coalescence). Off-diagonal peaks indicate chemical exchange due to P inversion (**6B1**/**6B2**) or interconversion of rotamers through P–P bond rotation (**6R1**/**6R2**).

To evaluate the effects influencing the relative stability of N versus P isomers, quantum chemical studies were carried out. Initially, N- and P-substituted 1,3-azaphosphole derivatives substituted with –PH$_2$ groups were investigated (Figure 6). It was found that the N-substituted derivatives are planar cyclodelocalized ring systems with the substituent in the ring plane and more stable by approximately 11 kcal mol^{-1} than the P-substituted structures with pyramidal configuration at the ring phosphorus atom.

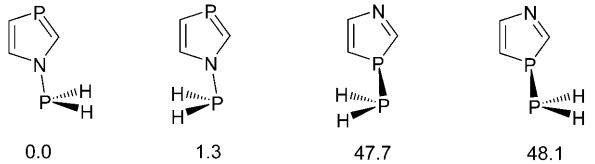

Figure 6. Possible phosphanylazaphosphole isomers (relative energies in kJ mol^{-1}, at the B3LYP/6-311+G** level).

Extending the aromatic system by attachment of a benzene ring to the 1,3-benzazaphosphole and substitution with the more bulky di-*tert*-butylphosphanyl group instead of –PH$_2$ caused a slight destabilization of the N- with respect to the P-substituted isomers, however, they are still more stable than the latter (Figure 7). The bulky N-substituent causes notable energetic differences of the two minimum energy rotamers with intersecting conformations and prefer the orientation of the *tert*-butyl groups at the free C2 side, whereas in the case of P-substitution the differences between the energies of the rotamers are smaller.

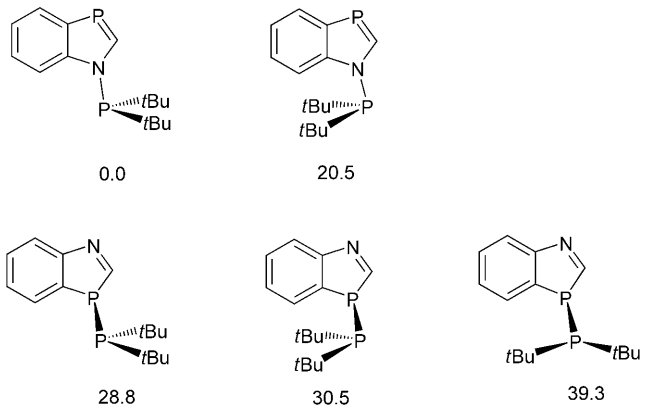

Figure 7. Possible (di-*tert*-butylphosphanyl)benzazaphosphole isomers (B3LYP/6-311+G**level, relative energies in kJ mol^{-1}).

Introduction of additional methyl groups in position 2 and 5, as present in **6**, resulted in further destabilization of the *N*-tBu$_2$P rotamers, and the *P*-tBu$_2$P-substituted systems become the more stable isomers. The computed inversion barrier about the ring phosphorus is 55 kJ mol^{-1}, whereas it is 85.2 kJ mol^{-1} about the exocyclic phosphorus. Although the computed inversion about the ring phosphorus is higher than the experimental value, it is still significantly lower than for phosphole (75.1 kJ mol^{-1}).[22] For these rotamers ^{31}P NMR spectroscopic shifts and coupling constants have also been calculated, and the values obtained are given in Figure 8. Relative stabilities and coupling constants are in good agreement with the experimental results. ^{31}P chemical shifts cannot be obtained with good accuracy by these calculations, but the trends are correct. Finally, it should be mentioned that, quite unexpectedly, the presence of the 2-methyl group is crucial to determine the regioselectivity of the phosphanylation with the bulky ligands.

The reduction of steric bulk at the phosphanyl group results in destabilization of the P- in favor of the N-substituted rotamers. This is seen by replacement of the tBu$_2$P with the iPr$_2$P or the sterically comparable dicyclohexylphosphanyl

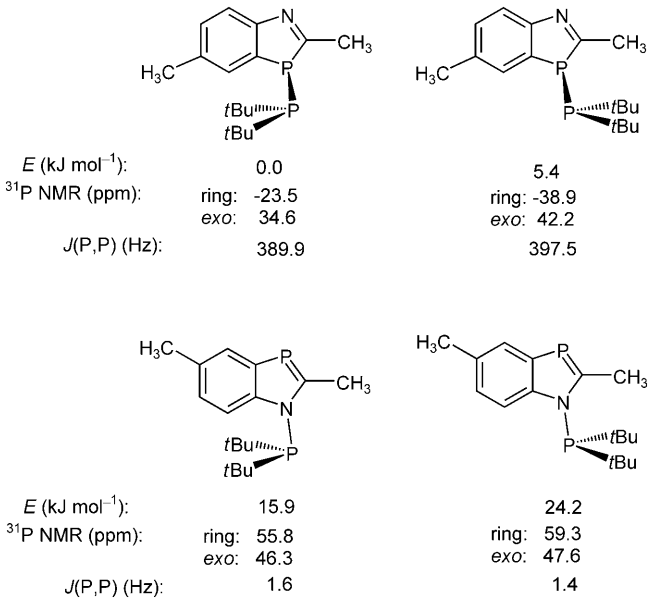

Figure 8. Relative energies of conformational isomers of **6** and its N-substituted counterparts (B3LYP/6-311+G**level, NMR spectroscopic data calculated at the B3LYP/6-31+G* level).

substituent. For these substituents, the N-substituted rotamers turned out to be slightly more stable than the *P*-phosphanyl rotamers (Figure 9), although the energy difference is very small.

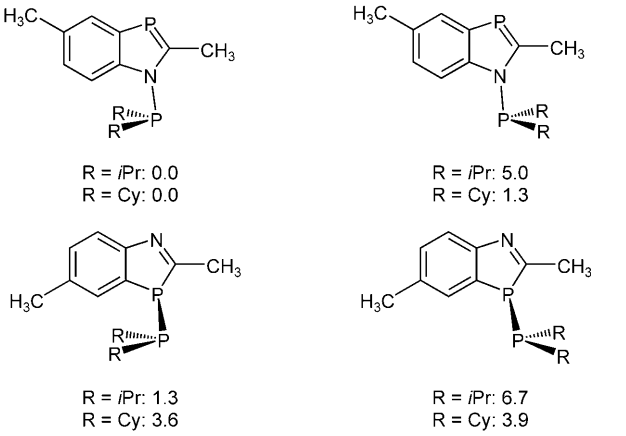

Figure 9. Relative energies of conformational isomers of diisopropylphosphanyldimethylbenzazaphosphole and **5** and its P-substituted counterparts (relative energies at the B3LYP/6-311+G**level, in kJ mol^{-1}).

The preference of N-substitution by less-bulky phosphanyl groups is attributable to the aromatic stabilization of these isomers, and the difference between the P–N and P–P bond strengths. In the P-substituted benzazaphospholes, the phosphorus atom is pyramidalized, and thus the lone pair of phosphorus cannot be involved in cyclic delocalization. The reason for the preference for *P*-phosphanylation in the case of bulky phosphanyl groups is that the steric encumbrance is alleviated by means of the relatively long P–P distance compared to the relatively short P–N distance in N-substituted compounds in the most stable di-*tert*-butylphosphanyl-2,5-dimethylbenzazaphosphole isomers (2.248 versus 1.797 Å). The introduction of a substituent at the 2-position plays a crucial role in the destabilization of the bulky *N*-phosphanylated benzazaphospholes and is responsible for the reversal of the stability order because the most suitable conformation with the phosphanyl substituents directed to the 2-CH side is destabilized.

Thus, the chemoselectivity of the phosphanylation of benzazaphospholides is governed by the interplay of aromatic stabilization and steric destabilization of the *N*-phosphanylated benzazaphospholes and the resulting delicate balance of energetically similar P- and N-substituted isomers. Small changes in the substitution pattern can affect the preferred chemoselectivity. Introduction of substituents with switchable space demand, either in the 2-position or the phosphanyl group, might allow switching between N- and P-substituted benzazaphospholes and an associated response in terms of their different electronic and spectral properties.

Conclusion

1,3-Benzazaphospholides, benzoanellated diheterocyclopentadienides, react with electrophiles at either of the two heteroatoms, nitrogen or phosphorus. In a first approximation this may be explained by the HSAB principle. The detailed investigation of the reaction with chlorophosphanes shows, however, a more sophisticated behavior. The substitution at nitrogen or phosphorus is controlled in a subtle way by electronic and steric factors. In the absence of steric hindrance, the phosphanylation takes place at nitrogen, as the planar N-substituted benzazaphospholes profit energetically from the formation of a heteroaromatic system, whereas P-substituted benzazaphospholes with pyramidal phosphorus are incapable of full electronic cyclodelocalization. Substituents at the 2-position of benzazaphospholides, even the small methyl group, disfavor N-substitution, however, particularly by bulky groups. The shorter bond of nitrogen than of phosphorus to the substituent causes much stronger hindrance for N- than P-substitution and energetic destabilization. This hindrance changes also the preferred conformation of the N-substituent. In 2-unsubstituted benzazaphospholes the substituents of the phosphanyl group are directed towards the five-membered ring end of the benzazaphosphole system, in the case of a 2-substituent towards the opposite site, the benzo-end. The knowledge of the factors governing N- or P-substitution of benzazaphospholides presented in this contribution may help pre-evaluate the role of steric factors governing the chemoselectivity in substitution reactions of ambident anions.

Experimental Section

General remarks: All reactions were carried out in heat-dried glass vessels under dry nitrogen or argon using Schlenk techniques and freshly distilled, ketyl-dried solvents. NMR spectroscopy solvents were dried (C_6D_6 and [D_8]THF over $LiAlH_4$, $CDCl_3$ over P_4O_{10}) and recondensed before use. Me_3SiCl was also recondensed under vacuum. Dicyclohexyl-,[23] di-*tert*-butyl-[24] and di-1-adamantylchlorophosphane[25] were prepared by known procedures. Other chemicals were used as purchased. NMR spectra were recorded using Bruker ARX300 or Avance 300 NMR spectrometers at 300.1 (^{1}H), 75.5 (^{13}C), and 121.5 MHz (^{31}P) (Greifswald), or using an Avance400 spectrometer at 400.13 (^{1}H) and 121.9 MHz (^{31}P) (Stuttgart). Shift references are tetramethylsilane for ^{1}H and ^{13}C and 85% H_3PO_4 (Ξ=40.480747 MHz) for ^{31}P. Coupling constants refer to *J*(H,H) in ^{1}H and *J*(P,C) in ^{13}C NMR spectroscopic data unless stated otherwise, and are given as absolute values. Assignments are supported by additional distortionless enhancement by polarization transfer (DEPT) measurements and further experiments described in the text. Assignment numbers are given in Scheme 1. The assignment C_q represents a quaternary carbon center. Mass spectra were recorded using a single-focusing mass spectrometer AMD40 (Intectra). HRMS measurements were carried out in Göttingen using a double-focusing sector-field instrument MAT 95 (Finnigan) with electron impact ionization (EI; 70 eV), or a 7 T Fourier transform ion cyclotron resonance mass spectrometer APEX IV (Bruker Daltonics) with electrospray ionization (ESI; PFK as reference substances). Melting points were determined using a Sanyo Gallenkamp melting-point apparatus in capillaries (uncorrected). Elemental analyses were performed using a Perkin–Elmer 24000CHN/O analyzer.

Compound 1: This compound, ^{31}P($CDCl_3$): δ=71.8 ppm, was prepared as reported earlier.[15a] Single crystals were grown from **1** in a THF/hexane mixture. Crystal data are compiled in Table 2.

Compound 3: Compound **2**[14] (1.16 g, 3.00 mmol) was dissolved in THF (20 mL) and cooled to −78 °C. Then a solution of $\mathbf{1_{Li}}$, prepared from **1** (0.55 g, 3.37 mmol) and the equimolar amount of *t*BuLi solution in THF (10 mL) at −78 °C, was slowly added. The mixture was allowed to warm to room temperature and stirred for 1 h. The solvent was removed under vacuum and the residue was extracted with toluene (30 mL). After filtration through Celite, the solution was concentrated under vacuum to about 5 mL and the precipitate was dissolved by addition of THF (3 mL). Yellow crystals, formed at +4 °C, were collected by filtration and dried under vacuum to give **3** (1.01 g, 64%). M.p. 147 °C; ^{1}H NMR (C_6D_6): δ=1.57 (s, 6H; 2Me), 1.66 (s, 6H; 2Me), 2.00 (s, 6H; 2Me), 2.10 (s, 6H; 2Me), 2.31 (s, 3H; 5-Me), 2.68 (dd, ^3J(P,H)=14.8 Hz, ^4J(P,H)=7.0 Hz, 3H; 2-Me), 6.49 (s, 2H; *m*-H), 6.73 (s, 2H; *m*-H), 7.21 (d, ^1J=8.6 Hz, 1H; H-6), 7.83 (d, ^3J(P,H)=4.3 Hz, 1H; H-4), 7.94 ppm (d, ^1J=8.6 Hz, 1H; H-7); ^{13}C{^{1}H} NMR (C_6D_6): δ=10.5 (d, ^3J=2.0 Hz; NC-CH_3), 18.9 (s; *p*-CH_3), 19.3 (d, ^4J=3.2 Hz; *o*-CH_3), 20.5 (d, ^4J=0.5 Hz; *o*-CH_3), 20.3 (dd, ^2J=28.1 Hz, ^3J=40.1 Hz; 2-Me), 21.0 (5-Me), 118.8 (s; CH-7), 120.5 (d, ^2J=6.3 Hz; N-C=), 125.7 (d, ^4J=2.5 Hz; CH-6), 128.7 (dd, ^2J=22 Hz, ^4J=1 Hz; CH-4), 129.1 (s; *m*-CH), 129.7 (d, ^3J=11.2 Hz; C_q-5), 130.1 (d, ^4J=2.0 Hz; *m*-CH), 135.3 (d, *J*=21.0 Hz; *o*-C_q or *i*-C_q), 137.0 (d, ^5J=2.0 Hz; *p*-C), 138.0 (d, *J*=3.6 Hz; *o*-C_q or *i*-C_q), 139.6 (d, *J*=3.6 Hz; *o*-C_q or *i*-C_q), 144.1 ppm (dd, ^2J=4.5, 7.7 Hz; C_q-7A); C_q-2 and C_q-3A were not detected; ^{31}P{^{1}H} NMR (C_6D_6): δ=90.5 (d, ^3J(P,P)=3.1 Hz; 3-P); 86.0 ppm (br s; N_2P); MS (EI, 70 eV, 490 K): *m*/*z* (%): 512.2 (0.1) $[M-1]^+$, 351.2 (100.0) $[M-C_9H_9NP]^+$, 163.1 (9.4) $[M-C_{22}H_{28}N_2P]^+$, 119.1 (2.3) $[M-C_{22}H_{26}N_3P_2]^+$; elemental analysis calcd (%) for $C_{31}H_{37}N_3P_2{\cdot}C_6H_6$: C 75.10, H 7.32, N 7.10; found: C 75.05, H 7.56, N 6.96.

Compound 4: *t*BuLi (0.58 mL 1.7 M in pentane, 0.99 mmol) was added dropwise to a solution of **1** (145 mg, 0.89 mmol) in THF (2 mL) at −78 °C. This mixture was stirred for 5 h while slowly warming up to −40 °C, then again cooled to −78 °C, and Ph_2PCl (0.16 mL, 0.889 mmol) was added dropwise. After stirring at room temperature overnight, THF was removed under vacuum and the residue was extracted with diethyl ether. Evaporation of the solvent gave an orange yellow viscous oil. The ^{31}P NMR (C_6D_6) spectrum displayed a mixture of products that included doublets indicating **4** by typical chemical shift and ^3J(P,P) coupling values (δ=40.5 (d, ^3J=6.9 Hz; Ph_2P), 92.9 ppm (d, ^3J=7.0 Hz; 3-P)), content 42 mol% of benzazaphospholes by integration of methyl protons. The methyl groups of **4** appear in the ^{1}H NMR ($CDCl_3$) spectrum at δ=2.12 (s; 5-Me) and 2.77 ppm (dd, *J*(P,H)=14.7, 1.9 Hz; 2-Me); aryl protons are superimposed. Further strong signals indicate **1** (δ(^{31}P)=73.7 ppm; δ(^{1}H)=2.21 (d, ^3J(P,H)=12.1 Hz; 2-Me), 2.29 ppm (s; 5-Me), content 42 mol% of benzazaphospholes) and at δ(^{31}P)=−14.8 ppm (Ph_2P-PPh_2). Weaker singlets are observed at δ(^{31}P)=116.9, 86.7 (w, m; both unknown), 17.9 ppm (w; *t*BuPPh_2), and −5.55 and −5.74 ppm, each with half intensity of the Ph_2P-PPh_2 signal. *t*Bu proton signals of *t*BuPPh_2 are observed at δ(^{1}H)=1.15 ppm (d, ^3J(P,H)=12.3 Hz).

Table 2. Crystallographic data.

	1	**3**	**5**	[**7**·LiCl(thf)]$_2$
formula	$C_9H_{10}NP$	$C_{37}H_{37}D_6N_3P_2$	$C_{21}H_{31}NP_2$	$C_{66}H_{94}Cl_2Li_2N_2O_2P_4$
M_r	163.15	597.70	359.41	1156.09
T [K]	133(2)	173(2)	100(2)	103(2)
λ [Å]	0.71073	0.71073	1.54184	1.54184
crystal system	monoclinic	monoclinic	monoclinic	triclinic
space group	*Pc*	$P2_1/c$	$P2_1/n$	$P\bar{1}$
a [Å]	8.3117(8)	17.673(3)	11.6572(3)	11.1411(6)
b [Å]	5.7552(4)	9.0335(13)	10.6438(3)	11.6873(12)
c [Å]	8.8751(8)	21.343(4)	16.3790(4)	12.9262(8)
α [°]	90	90	90	77.481(6)
β [°]	98.927(4)	90.863(14)	94.812(2)	83.739(6)
γ [°]	90	90	90	66.133(6)
V [Å^3]	419.40(6)	3407.0(10)	2025.09(9)	1502.2(2)
Z	2	4	4	1
ρ_{calcd} [Mg m^{-3}]	1.292	1.165	1.179	1.278
μ [mm^{-1}]	0.257	0.156	1.944	2.327
F(000)	172	1264	776	620
crystal size [mm^3]	0.4×0.3×0.3	0.7×0.45×0.2	0.35×0.15×0.04	0.10×0.08×0.03
θ range [°]	2.48 to 30.56	2.21 to 27.00	4.48 to 71.14	3.50 to 71.09
index ranges	$-11 \le h \le 11$	$0 \le h \le 22$	$-13 \le h \le 14$	$-9 \le h \le 13$
	$-8 \le k \le 8$	$0 \le k \le 11$	$-13 \le k \le 13$	$-14 \le k \le 13$
	$-12 \le l \le 12$	$-27 \le l \le 27$	$-20 \le l \le 19$	$-15 \le l \le 15$
collected reflns	6139	7687	57680	28262
independent reflns	2495	7447	3849	5559
R(int)	0.0154	0.0451	0.0341	0.0291
completeness to θ [°]	30.00 (99.5%)	27.00 (99.9%)	67.50 (99.9%)	67.50 (98.4%)
max/min transmission	0.9270/0.8145	–	1.00000/0.68127	1.00000/0.75697
data/restraints/params	2495/2/107	7447/0/379	3849/0/219	5559/0/354
GOF on F^2	1.106	0.866	1.072	1.033
final R indices	$R1$=0.0338	$R1$=0.0624	$R1$=0.0447	$R1$=0.0348
($I>2\sigma(I)$)	$wR2$=0.0836	$wR2$=0.1611	$wR2$=0.1114	$wR2$=0.0954
R indices	$R1$=0.0343	$R1$=0.1020	$R1$=0.0478	$R1$=0.0415
(all data)	$wR2$=0.0842	$wR2$=0.1740	$wR2$=0.1140	$wR2$=0.1000
largest diff. peak/hole [e Å^{-3}]	0.597/−0.184	0.961/−0.491	1.027/−0.582	0.545/−0.307

Compound 5: Chlorodicyclohexylphosphane (0.64 mL, 2.897 mmol) was added dropwise at −78 °C to a solution of $\mathbf{1_{Li}}$, prepared from **1** (450 mg, 2.76 mmol) in THF (5 mL) and *t*BuLi (2.02 mL, 3.03 mmol, 1.5 M in pentane) as described above. After stirring overnight at room temperature THF was removed under vacuum. The residue was extracted with hexane yielding a yellow crystalline slush. This mixture was purified by crystallization from a mixture of THF/hexane to give colorless solid **5** (465 mg, 47 %) . NMR spectra at 25 °C in C_6D_6 indicate two sets of signals, ratio by ^{1}H integration of methyl signals approximately 90–85:10–15 mol %. ^{1}H NMR (C_6D_6): *major rotamer*: δ = 0.8–1.72 (5 m, 20 H; PCy_2), 2.25 (s, 3 H; 5-Me), 2.69 (m, 2 H; PCH_α), 2.95 (dd, ^3J(P,H) = 14.4 Hz, ^4J(P,H) = 3.4 Hz, 3 H; 2-Me), 7.09 (dd, ^3J = 8.6 Hz, ^4J = 1.6 Hz, 1 H; H-6), 7.68 (d, ^3J = 8.6 Hz, 1 H; H-7), 7.80 ppm (dd, ^3J(P,H) = 4.6 Hz, ^4J = 1.6 Hz, 1 H; H-4); *minor rotamer*: δ = 2.27 (s; 5-Me), 2.62 (d, ^3J(P,H) = 14.9 Hz; 2-Me), 7.17 (dd, $^3J \approx 8$ Hz, $^4J \approx 2$ Hz; H-6), 7.80 (superimposed d; H-4), 8.49 ppm (dd, ^3J = 8.7 Hz, ^4J(P,H) = 4.5 Hz; H-7); cyclohexyl superimposed; ^{13}C{^{1}H} (DEPT) NMR (C_6D_6): *major rotamer*: δ = 20.95 (s; 5-Me), 21.67 (dd, ^2J = 27.4 Hz, ^3J = 31.4 Hz; 2-Me), 26.23 (s; CH_2-δ), 26.32 (d, ^3J = 6.8 Hz; CH_2-γ), 26.47 (CH_2-γ), 28.89 (d, ^2J = 9.4 Hz; CH_2-β), 30.99 (d, ^2J = 29.5 Hz; CH_2-β), 36.18 (d, ^1J = 18.7 Hz; CH-α), 115.03 (s; CH-7), 125.70 (d, ^4J = 2.4 Hz; CH-6), 129.48 (d, ^2J = 21.8 Hz; CH-4), 130.12 (d, ^3J = 10.8 Hz; C_q-5), 142.95 (d, ^1J = 36.2 Hz; C_q-3A), 145.79 (dd, ^2J = 9.3 Hz, J = 5.1 Hz; C_q-7A), 184.59 ppm (dd, ^1J = 47.6 Hz, ^2J = 19.3 Hz; C_q-2); *minor rotamer*: δ = 19.90 (d, ^2J = 29.4 Hz; 2-Me), (5-Me, CH_2-δ, CH_2-γ superimposed), 28.65 (d, ^2J = 8.0 Hz; CH_2-β), 31.38 (d, ^2J = 29.5 Hz; CH_2-β), 38.04 (d, ^1J = 18.7 Hz; CH-α), 116.92 (d, ^3J = 33.3 Hz; CH-7), 125.99 (t, ^4J = 2.6 Hz; CH-6), 128.04 (d, ^2J = 21.1 Hz; CH-4), 129.78 (d, ^3J = 12.9 Hz; C_q-5), 142.38 (d, ^1J = 34.6, ^3J = 3.9 Hz; C_q-3A), 150.72 (dd, ^2J = 24.1, 5.1 Hz; C_q-7A), 180.75 ppm (dd, ^1J = 48.7 Hz, ^2J = 11.8 Hz; C_q-2); ^{31}P{^{1}H} NMR (C_6D_6): *major rotamer*: δ = 61.5 (d, ^3J(P,P) = 7.3 Hz; PCy_2), 85.20 ppm (d, ^1J(P,P) = 7.9 Hz; P-3); *minor rotamer*: δ = 64.6 (br s; PCy_2), 95.17 ppm (d, ^1J(P,P) = 4.2 Hz; P-3); trace 73.2 ppm (**1**); HRMS (ESI in MeOH/NH_4): m/z calcd for $C_{21}H_{31}NP_2$ $[M+H]^+$: 360.20045; found: 360.20042 (low intensity by decomposition).

Compound 6: Di(*tert*-butyl)chlorophosphane (0.25 mL, 1.46 mmol) was added dropwise at −78 °C to a solution of $\mathbf{1_{Li}}$, prepared from **1** (200 mg, 1.23 mmol) in THF (2 mL) and *t*BuLi (0.9 mL, 1.35 mmol, 1.5 M in pentane) as described above. The mixture was stirred at room temperature overnight. THF was removed from the reaction mixture under vacuum, the residue was extracted with hexane, and hexane was evaporated under vacuum to give a yellow viscous oil. NMR spectroscopic control (C_6D_6) showed that the oil consisted mainly of **6**, contaminated by small amounts of impurities. One crystallized and proved crystallographically identical to *t*Bu_2PHO·LiCl.[26] The oil was separated and purified by high-vacuum distillation at 60 °C bath temperature, b.p. around 30 °C/1.1×10^{-5} mbar, to give a colorless oil (233 mg, 62 %). ^{1}H NMR (C_6D_6): δ = 1.12 (br d, ^3J(P,H) = 12.4 Hz, 18 H; $PCMe_3$), 2.18 (s, 3 H; 5-Me), 2.76 (d, ^3J(P,H) = 9.2 Hz, 3 H; 2-Me), 7.03 (dd, ^3J = 8.1 Hz, ^4J = 1.5 Hz, 1 H; H-6), 7.72 (br s, 1 H; H-4), 8.02 ppm (d, ^3J = 8.1 Hz, 1 H; H-7); ^{13}C{^{1}H} (DEPT) NMR (C_6D_6): δ = 21.28 (s; 5-Me), 21.80 (dd, ^2J = 25.1 Hz, ^3J = 3.6 Hz; 2-Me), 31.38 (dd, ^2J = 13.3 Hz, ^3J = 5.2 Hz; CMe_3), 36.64 (vbr d, J = 26.3 Hz; C_qMe_3), 124.71 (s; CH-7), 129.23 (d, ^2J = 18.6 Hz; CH-4), 129.81 (s; CH-6), 134.16 (d, ^3J = 6.6 Hz; C_q-5), 135.39 (br d, ^1J = 9.7 Hz; C_q-3A), 156.59 (br d, ^2J = 14.8 Hz; C_q-7A), 184.89 ppm (dd, $^1J \approx 25$ Hz, ^2J = 9.7 Hz; C_q-2); ^{31}P{^{1}H} NMR (C_6D_6): δ = −6.0 (d, ^1J(P,P) = 425 Hz; 3-P), 46.4 (br d, ^1J(P,P) = 430 Hz); small hydrolysis impurities at 61.9 (*t*Bu_2PHO) and 73.5 ppm (**1**); MS (EI, 70 eV, 50 °C): m/z: calcd (%) for $C_{17}H_{27}NP_2$ (307.16): 308 (2), 307 (10) [M^+], 250 (6), 194 (34), 57 (100); HRMS after short air contact (ESI in MeOH): m/z calcd for $[C_{17}H_{27}NP_2+O+H^+]$: 324.16406; found: 324.16406 [M^++OH]; (ESI in MeOH, CH_3COONa): m/z calcd for $[C_{17}H_{27}NP_2+O+Na^+]$: 346.14601; found: 346.14631.

Compound [7]: Di(1-adamantyl)chlorophosphane (2.3 g, 6.83 mmol) was added dropwise at −78 °C to a solution of $\mathbf{1_{Li}}$, prepared from **1** (1.11 g, 6.80 mmol) in THF (10 mL) and *t*BuLi (4.7 mL, 7.52 mmol, 1.6 M in pentane) as described above, and stirred at room temperature. The solution turned slowly from yellow to orange. Reaction control showed that after three weeks at room temperature the major part of the starting materials had reacted. THF was removed under vacuum to give an orange semicrystalline crude product (2.7 g). The ^{31}P NMR spectra displayed broad doublets of the product and contamination by small amounts of unconverted $\mathbf{1_{Li}}$ ($\delta(^{31}P)$ = 56.7 ppm) and Ada_2PCl ($\delta(^{31}P)$ = 139.8 ppm), and traces of two unknown phosphorus compounds ($\delta(^{31}P)$ = 18.2, 83.7 ppm). An attempt at high-vacuum distillation (separate experiment) led to thermal decomposition. Overlayering of a concentrated solution of crude **7** in THF by hexane gave crystals of $[\mathbf{7}\cdot LiCl(THF)]_2$, thus allowing a structure analysis. The crystal data are compiled in Table 2. ^{1}H NMR (C_6D_6): δ = 1.50, 1.58, 1.72–1.85, 1.90–2.10 (m, 30 H; ada), 2.22 (s, 3 H; 5-Me), 2.84 (d, ^3J(P,H) = 9.3 Hz, 3 H; 2-Me), 7.07 (dd, ^3J = 7.8 Hz, ^4J = 1.1 Hz, 1 H; H-6), 7.87 (br s, 1 H; H-4), 8.06 ppm (d, ^3J = 8.0 Hz, 1 H; H-7); ^{13}C{^{1}H} (DEPT) NMR (C_6D_6): δ = 21.37 (s; 5-Me), 21.84 (br d, ^2J = 25.8 Hz; 2-Me), 25.80 (s; CH_2[THF]), 29.26 (d, ^3J = 8.3 Hz; 3 CH), 36.71 (s; 3 CH_2), 41.61 (vbr d, ^1J = 30.9 Hz; C_q-1), 42.88 (dd, ^2J = 10.2 Hz, ^3J = 6.0 Hz; CH_2), 67.80 (s; CH_2[THF]), 124.69 (s; CH-7), 129.27 (d, ^2J = 19.6 Hz; CH-4), 129.49 (s; CH-6), 133.78 (d, ^3J = 5.3 Hz; C_q-5), 136.2 (br; C_q-3A), 156. 7 (br; C_q-7A), 186.3 ppm (vbr; C_q-2); ^{31}P{^{1}H} NMR (C_6D_6): δ = −12.3 (br d, ^1J(P,P) = 418 Hz; 3-P), 39.4 ppm (br d, ^1J(P,P) ≈ 410 Hz); HRMS of uncoordinated **7** (ESI in MeCN): m/z calcd for $[C_{29}H_{39}NP_2+H]^+$: 464.26305; found: 464.26285; elemental analysis calcd (%) for $C_{66}H_{94}Cl_2Li_2N_2O_2P_4$ (1156.15): C 68.56, H 8.20, N 2.42; found: C 68.35, H 8.43, N 2.26.

Crystal-structure analyses: Selected data collection parameters and other crystallographic data are summarized in Table 2.

Data collection and reduction: All measurements were carried out at low temperature using crystals mounted in inert oil on glass fibers. Compound **1** was measured using a Bruker SMART 1000 CCD; compound **3** using a Siemens P4 diffractometer (both with $Mo_{K\alpha}$ radiation); compound **5** and $[\mathbf{7}\cdot LiCl(thf)]_2$ using an Oxford Diffraction Nova diffractometer with $Cu_{K\alpha}$ radiation. Data for **3** were not corrected for absorption effects; for the other structures, absorption corrections (semiempirical from equivalents) were applied on the basis of multiscans.

Structure solution and refinement: Structures were solved by direct methods and refined on F_O^2 by full-matrix least-squares refinement using the SHELX suite of programs.[27] Hydrogen atoms were included using a riding model or with rigid methyl groups.

Exceptions and special features: For **1**, the NH hydrogen was refined freely; the structure was refined as a racemic twin with components 0.56, 0.44(7). For **3**, the carbon atoms of the cocrystallized deuterobenzene molecule were constrained to a regular hexagon.

CCDC-734965 (**1**), 726723 (**3**), 734966 (**5**), and 734967 ($[\mathbf{7}\cdot LiCl(thf)]_2$) contain the supplementary crystallographic data for this paper. These data can be obtained free of charge from The Cambridge Crystallographic Data Centre via www.ccdc.cam.ac.uk/data_request/cif.

Quantum chemical calculations: All calculations were carried out with the Gaussian 03 program package.[28] Full geometry optimizations were performed for all examined molecules at the B3LYP/6-311+G** level,[29] and vibrational frequencies were calculated to establish the nature of stationary points obtained. ^{31}P NMR spectroscopic shifts (using tetramethylsilane and gas-phase PH_3 as reference[30]) and P,P coupling constants were calculated at the B3LYP/6-31+G*//B3LYP/6-311+G** level.

Acknowledgements

Financial support and a fellowship (B.R.A.) from the Deutsche Forschungsgemeinschaft is gratefully acknowledged. We thank B. Witt, W. Heiden, and M. Steinich for NMR and mass spectra, and Dr. H. Frauendorf and G. Sommer-Udvarnoki (Georg-August-Universität Göttingen, Institut für Organische und Biomolekulare Chemie) for HRMS measurements. D.G. and L.N. acknowledge the financial support from DFG-HAS and COST CM0802.

[1] J. Heinicke, *Tetrahedron Lett.* **1986**, *27*, 5699–5702.

[2] a) A. Schmidpeter in *Comprehensive Heterocyclic Chemistry II* (Eds.: R. Katritzky, C. W. Rees, E. F. V. Scriven), Pergamon, Oxford, **1996**, Chapter 4.22; b) A. Schmidpeter in *Phosphorus-*

Carbon Heterocyclic Chemistry: The Rise of a New Domain (Ed.: F. Mathey), Pergamon, Amsterdam, **2001**, pp. 363–461; c) R. K. Bansal, J. Heinicke, *Chem. Rev.* **2001**, *101*, 3549–3578.

[3] a) L. Szarvas, Z. Bajko, S. Fusz, S. Burck, J. Daniels, M. Nieger, D. Gudat, *Z. Anorg. Allg. Chem.* **2002**, *628*, 2303–2310; b) G. Märkl, I. Trötsch, *Angew. Chem.* **1984**, *96*, 899–900; c) J. G. Kraaijkamp, D. M. Grove, G. van Koten, A. Schmidpeter, *Inorg. Chem.* **1988**, *27*, 2612–2617.

[4] a) "Metallocene complexes as catalysts for olefin polymerization": *Coord. Chem. Rev.* **2006**, *250*, 1–272, edited by H. G. Alt; b) "Metallocenes in regio- and stereoselective synthesis": *Top. Organomet. Chem.* **2005**, *8*, 1–244, edited by T. Takahashi.

[5] T. Veszprémi, J. Mátrai, J. Heinicke, M. K. Kindermann, *J. Mol. Struct.* **2001**, *559*, 189–195.

[6] a) A. Surana, S. Singh, R. K. Bansal, N. Peulecke, A. Spannenberg, J. Heinicke, *J. Organomet. Chem.* **2002**, *646*, 113–124; b) J. Heinicke, A. Surana, N. Peulecke, R. K. Bansal, A. Murso, D. Stalke, *Eur. J. Inorg. Chem.* **2001**, 2563–2567.

[7] K. Issleib, R. Vollmer, *Z. Anorg. Allg. Chem.* **1981**, *481*, 22–32.

[8] J. Heinicke, A. Petrasch, A. Tzschach, *J. Organomet. Chem.* **1983**, *258*, 257–269.

[9] A. Schmidpeter, H. Tautz, *Z. Naturforsch. B* **1980**, *35*, 1224–1228.

[10] a) L. Nyulászi, G. Csonka, J. Réffy, T. Veszprémi, J. Heinicke, *J. Organomet. Chem.* **1989**, *373*, 49–56; b) L. Nyulászi, G. Csonka, J. Réffy, T. Veszprémi, J. Heinicke, *J. Organomet. Chem.* **1989**, *373*, 57–61; c) T. Veszprémi, L. Nyulászi, J. Reffy, J. Heinicke, *J. Phys. Chem.* **1992**, *96*, 623–626; d) L. Nyulászi, T. Veszprémi, J. Réffy, B. Burkhardt, M. Regitz, *J. Am. Chem. Soc.* **1992**, *114*, 9080–9084; e) L. Nyulaszi, *Chem. Rev.* **2001**, *101*, 1229–1246.

[11] S. Burck, D. Gudat, M. Nieger, *Angew. Chem.* **2004**, *116*, 4905–4908; *Angew. Chem. Int. Ed.* **2004**, *43*, 4801–4804.

[12] S. Burck, D. Gudat, M. Nieger, D. Vindus, *Eur. J. Inorg. Chem.* **2008**, 704–707.

[13] S. Burck, D. Gudat, M. Nieger, *Angew. Chem.* **2007**, *119*, 2977–2980; *Angew. Chem. Int. Ed.* **2007**, *46*, 2919–2922.

[14] a) S. Burck, D. Gudat, M. Nieger, Z. Benkö, L. Nyulaszi, D. Szieberth, *Z. Anorg. Allg. Chem.* **2009**, *635*, 245–252; b) S. Burck, D. Gudat, K. Naettinen, M. Nieger, M. Niemeyer, D. Schmid, *Eur. J. Inorg. Chem.* **2007**, 5112–5119; c) D. Gudat, A. Haghverdi, H. Hupfer, M. Nieger, *Chem. Eur. J.* **2000**, *6*, 3414–3425.

[15] a) J. Heinicke, N. Gupta, A. Surana, N. Peulecke, B. Witt, K. Steinhauser, R. K. Bansal, P. G. Jones, *Tetrahedron* **2001**, *57*, 9963–9972; b) R. K. Bansal, N. Gupta, J. Heinicke, G. N. Nikonov, F. Saguitova, D. C. Sharma, *Synthesis* **1999**, 264–269.

[16] G. Becker, W. Massa, O. Mundt, R. E. Schmidt, C. Witthauer, *Z. Anorg. Allg. Chem.* **1986**, *540/541*, 336–344.

[17] S. Burck, D. Gudat, F. Lissner, K. Naettinen, M. Nieger, T. Schleid, *Z. Anorg. Allg. Chem.* **2005**, *631*, 2738–2745.

[18] a) B. Gehrhus, P. B. Hitchcock, M. F. Lappert, *J. Chem. Soc. Dalton Trans.* **2000**, 3094–3099; b) W. M. Boesfeld, B. Gehrhus, P. B. Hitchcock, M. F. Lappert, P. von R. Schleyer, *Chem. Commun.* **1999**, 755–756; c) F. E. Hahn, L. Wittenbecher, M. Kühn, T. Lügger, R. Fröhlich, *J. Organomet. Chem.* **2001**, *617–618*, 629–634.

[19] H. C. E. McFarlane, W. McFarlane, A. J. Nash, *J. Chem. Soc. Dalton Trans.* **1980**, 240–244.

[20] J. G. Verkade, J. A. Mosbo in *Phosphorus-31 NMR Spectroscopy in Stereochemical Analysis, Methods in Stereochemical Analysis, Vol. 8* (Eds.: J. G. Verkade, L. D. Quin), VCH, Weinheim, **1987**, p. 425.

[21] L. D. Quin in *Phosphorus-31 NMR Spectroscopy in Stereochemical Analysis, Methods in Stereochemical Analysis, Vol. 8* (Eds.: J. G. Verkade, L. D. Quin), VCH, Weinheim **1987**, p. 391.

[22] A. Dransfeld, L. Nyulaszi, P. v. R. Schleyer, *Inorg. Chem.* **1998**, *37*, 4413–4420.

[23] K. Issleib, W. Seidel, *Chem. Ber.* **1959**, *92*, 2681–3008.

[24] M. Fild, O. Stelzer, R. Schmutzler in *Inorganic Synthesis, Vol. 14* (Eds.: A. Wold, J. Ruff), McGraw-Hill, New York, **1973**, pp. 6–7.

[25] J. R. Goerlich, R. Schmutzler, *Phosphorus Sulfur Silicon Relat. Elem.* **1995**, *102*, 211–215.

[26] B. R. Aluri, M. K. Kindermann, P. G. Jones, I. Dix, J. W. Heinicke, *Inorg. Chem.* **2008**, *47*, 6900–6912.

[27] G. M. Sheldrick, *Acta Crystallogr. Sect. A* **2008**, *64*, 112–122.

[28] Gaussian 03, Revision C.02, M. J. Frisch, G. W. Trucks, H. B. Schlegel, G. E. Scuseria, M. A. Robb, J. R. Cheeseman, J. A. Montgomery, Jr., T. Vreven, K. N. Kudin, J. C. Burant, J. M. Millam, S. S. Iyengar, J. Tomasi, V. Barone, B. Mennucci, M. Cossi, G. Scalmani, N. Rega, G. A. Petersson, H. Nakatsuji, M. Hada, M. Ehara, K. Toyota, R. Fukuda, J. Hasegawa, M. Ishida, T. Nakajima, Y. Honda, O. Kitao, H. Nakai, M. Klene, X. Li, J. E. Knox, H. P. Hratchian, J. B. Cross, V. Bakken, C. Adamo, J. Jaramillo, R. Gomperts, R. E. Stratmann, O. Yazyev, A. J. Austin, R. Cammi, C. Pomelli, J. W. Ochterski, P. Y. Ayala, K. Morokuma, G. A. Voth, P. Salvador, J. J. Dannenberg, V. G. Zakrzewski, S. Dapprich, A. D. Daniels, M. C. Strain, O. Farkas, D. K. Malick, A. D. Rabuck, K. Raghavachari, J. B. Foresman, J. V. Ortiz, Q. Cui, A. G. Baboul, S. Clifford, J. Cioslowski, B. B. Stefanov, G. Liu, A. Liashenko, P. Piskorz, I. Komaromi, R. L. Martin, D. J. Fox, T. Keith, M. A. Al-Laham, C. Y. Peng, A. Nanayakkara, M. Challacombe, P. M. W. Gill, B. Johnson, W. Chen, M. W. Wong, C. Gonzalez, J. A. Pople, Gaussian, Inc., Wallingford CT, **2004**.

[29] a) A. D. Becke, *J. Chem. Phys.* **1993**, *98*, 5648; b) C. Lee, W. Yang, R. G. Parr, *Phys. Rev. B* **1988**, *37*, 785.

[30] C. van Wüllen, *Phys. Chem. Chem. Phys.* **2000**, *2*, 2137–2144.

Received: June 24, 2009
Published online: October 9, 2009

